IIETA International Information and Engineering Technology Association
Advancing the World of Information and Engineering

Journal of New Materials for Electrochemical Systems

Vol. 27, No. 3, September 2024, pp. 276-289

Journal homepage: http://iieta.org/journals/jnmes

Optimization and Characterization of Borassus Fiber-Reinforced Epoxy Composites with Caesalpinia Bonducella Seed Shell Powder Using Response Surface Methodology

R. Malairaja[1] and V. Vijayan[2]

[1] Assistant professor Department of Mechanical Engineering Muthayammal Engineering College (Autonomous) Rasipuram Namakkal 637 408
[2] Department of Mechanical Engineering, K. Ramakrishnan College of Technology, Tiruchirappalli – 621 112, Tamilnadu, India

Corresponding Author Email: Vijayan.me@gmail.com

https://doi.org/10.14447/jnmes.v27i3.a13

Received: 21/01/2024
Accepted: 23/08/2024

Keywords:
Borassus fibre, Caesalpinia bonducella, morphological analysis, RSM, Tensile properties, Flexural strength, and moisture absorption

ABSTRACT

Utilizing reinforced lignocellulosic fibers in polymer matrix composites (PMCs) is a highly effective approach, since it reduces the necessity for more often used synthetic fibers. To investigate the uses of particulate matrix composites (PMCs), we concentrated on studying the fibers from Borassus, which are underutilized and have not been well researched. In this study, we used particles of Caesalpinia bonducella seed shell powder (CBSSP) and Borassus fibers (BF) as a reinforcing agent. The research aimed to assess the effectiveness of different CBSSP and Borassus fibers (BF) through treatment with 5% NaOH. The use of alkali treatment to CBSSP and BF samples significantly improved the compatibility between the biomaterial's characteristics and the natural fillers in the epoxy-BF composites. This enhancement was noted in the findings of physicochemical, XRD, FTIR, thermal and morphological analysis. In response surface analysis, a first-degree polynomial model was employed to maximize tensile strength (TS), tensile modulus (TM), flexural strength (FS), impact energy (IE), and moisture absorption of reinforced fiber. The optimization was done by considering the composition and length of the fiber. The Response Surface methodology (RSM) numerical model was used to analyze the mentioned characteristics and develop an ideal Epoxy-BF composite with minimum moisture absorption, maximum tensile modulus, flexural strength, and impact energy. After analyzing the data, it was concluded that the most effective setup for the Epoxy-BF composite is to use a 4 mm fiber length reinforcement combined with a loading reinforcement of 25 wt % of biomaterials.

1. INTRODUCTION

Biocompatibility and degradation of naturally occurring cellulosic scaffolds made from bamboo fibers by means of surface functionalization and chemical oxidation[1]. The scaffolds exhibited desirable physicochemical characteristics and demonstrated better cellular proliferation and differentiation in laboratory settings and improved blood vessel formation and tissue restructuring in living organisms [2].The effect of two-step densification on the inner soft portion of Borassus flabellifer wood was investigated and it rendering the wood more suited for a wide range of applications [3].Palmyra fibers were extracted from Borassus flabellifer leaves and incorporated into cement composites at varying contents and lengths. Mechanical strength and water absorption tests were conducted to evaluate the composite performance [4].Pure cellulose nanofibers were extracted from Palmyra fruit fiber using alkaline treatment, bleaching, and acid hydrolysis. These nanofibers were then used to reinforce starch-based biodegradable films, which were evaluated for mechanical and water absorption properties [5].

Borassus flabellifer leaf fibers were treated with NaOH using varying concentrations and durations. The effects on water absorption, tensile strength, and morphology were analyzed using SEM and FTIR [6]. Nanocellulose was extracted from Borassus flabellifer husk using TEMPO-mediated oxidation and ultrasonication. The nanocellulose was incorporated into arrowroot starch-based films with neem oil, and the films were tested for mechanical, antioxidant, and antimicrobial properties [7]. Borassus Flabellifer Petiole and Leaf Stalk fibers were combined in a vinyl ester matrix to form hybrid composites with various stacking sequences. The composites were characterized for tensile strength, impact resistance, hardness, and water absorption [8]. Turbostratic-activated carbon was extracted from Borassus flabellifer inflorescence flowers,

followed by sulfonation with different sulfonating agents. The sulfonated carbon was used to coat Li-metal anodes to inhibit dendritic growth in Li-metal batteries [9]. Borassus fibers were reviewed for their potential use in polymer composites with an emphasis on alkali treatment techniques and various fabrication methods. The study also examined the mechanical, chemical, and thermal characteristics of these fibers and their composites [10].

Rice husk nanoparticles were blended with epoxy resin and reinforced with Borassus flabellifer leaf fiber. The erosion resistance of thecomposites was tested using an air jet test rig and analyzed using Taguchi method, ANOVA, and artificial neural networks [11]. The study evaluated the mechanical characteristics of composite materials made from Borassus flabellifer sprout fibers and polyester. Significant improvements in mechanical properties and reduced water absorption were seen in the fibers treated at a volume concentration of 35% [12]. The modified Borassus flabellifer fibers exhibited enhanced crystallinity, thermal stability, tensile strength, and reduced water absorption. The benzoyl chloride-treated fibers showed the best improvements in these properties, as confirmed by XRD, SEM, and Thermo-gravimetric analysis (TGA)[13]. The extracted microcrystalline cellulose from Borassus flabellifer flower showed a crystallinity index of 69.81%, a crystalline size of 70.73 nm, and thermal stability up to 200°C. The cellulose also exhibited low surface roughness and absence of lignin and hemicellulose [14]. The study examined the tensile strength, hardness, thermal stability, and moisture absorption of epoxy composites reinforced with Borassus leaf fibers and blended with rice husk nanoparticles. The composites containing 0.45 wt % of RHN demonstrated the most optimal combination of mechanical characteristics and thermal stability [15]. The palmyrah leaf base fibers had a tensile strength of 8.77 MPa, flexural strength of 147 MPa, and high hardness but reduced impact strength, indicating their viscoelastic properties. The properties underwent statistical investigation utilizing Weibull analysis [16].

The PLA-surface modified nano cellulose composite demonstrated a TS of 0.244 MPa, Young's modulus of 0.0030 GPa and a water contact angle of 117º. The composite demonstrated superior UV stability, biodegradability, and mechanical properties as compared to pure PLA [17]. The cellulose microfibrils (CMFs) derived from palmyra fruit peduncle waste have a crystallinity index of 78.2%, a TS of 693.3 MPa, and demonstrate remarkable thermal stabilization up to 330ºC. The findings suggest that CMFs has substantial potential as reinforcing agents in composites. [18]. The Borassus Flabellifer (BF) fibers treated with alkali showed improved mechanical capabilities, lower water absorption, and excellent thermal stability. These characteristics make them ideal for use in UAV landing gear applications, surpassing other composites made from natural fibers [19]. The Caesalpinia bonducella seed extracts showed significant antibacterial activity against multiple pathogens, with phytochemical analysis confirming the presence of active constituents, suggesting their potential as natural antibiotics [20].

The study found that Moringa oleifera seed powder achieved an 83% reduction in nematode egg count in goats, indicating strong anthelmintic properties comparable to commercial treatments [21]. The aqueous extract of C. bonducella showed significant anti-inflammatory activity, with 75% membrane stabilization and attenuation of nitric oxide, confirming the extract's potential for anti-inflammatory applications [22]. The extract from the Bonduc nuthad a substantial impact on antioxidant levels and lipid peroxidation in rats with spleen and heart damage caused by APAP. This suggests that BNE has protective benefits in these conditions [23]. A diverse range of bioactive compounds in the ethanolic extract of Caesalpinia bonducella leaves. This discovery provides evidence for the conventional application of the plant in the treatment of several illnesses and indicates its potential in contemporary medicine [24]. The hybrid composite, including alternating Sisal and PALF, exhibited a maximum TS of 70.8 MPa. The composite, which consisted of an exterior layer made of Sisal, had remarkable fracture toughness, measuring at 3302.3 J/m², along with an amazing interlaminar shear strength (ILSS) of 16.1 MPa [25]. The composite, comprising 12 wt% marble dust powder and 16 wt% coconut fiber exhibited the maximalTS (34.27 MPa), FS (37.23 MPa), and impact strength (16.32 kJ/m²). There was a little elevation in the rate of wear when the quantity of filler beyond 12 wt%[26]. The hybrid composite, composed of 2.5 wt % nano Al_2O_3 and 7.5 wt % arecanut shell powder, exhibited the greatest values for TS (49.37 MPa), yield strength (YS) (46.89 MPa), and compressive strength (CS) (46.71 MPa).[27].

The incorporation of Tamarindus indica seed powder into the sugarcane fiber with epoxy resin matrix significantly improved the tensile properties of the hybridized bio-composites [28]**.**The incorporation of fine granite powder and Tamarindus indica shell powder into the epoxy resin matrix greatly enhanced the CS of the hybridized bio-composites [29]. The composite material consisting of 35% sugarcane fiber and 15% tamarind seed powder had the highest flexural strength (36.543 MPa), flexural modulus (12.129 GPa), and compressive strength (21.32 MPa) [30]. The film composed of PLA-SMNC-ZnO nanoparticles, with a surface modified nano cellulose (SMNC) layer, demonstrated exceptional tensile strength (13.9 MPa) and Young's modulus (0.00689 GPa) as compared to films made only of PLA or PLA-SMNC. The film exhibited improved thermal stability at a temperature of 320°C, decreased water absorption, and improved resistance to UV radiation[31]. The composite with 35 wt% BF sprout fibers showed the best tensile strength (17.6 ± 0.72 MPa), flexural strength (50.2 ± 0.15 MPa), and impact strength (1.18 ± 0.21 J). The wear measurements revealed a COF of 0.52 and a SWR of 0.024 mm³/Nm, indicating a robust link between the surfaces [32].

This work aims to utilize the particles of Caesalpinia bonducella seed shell powder (CBSSP) for reinforcing purposes. The alkaline treatment is the most efficient technique for chemically altering natural fibers. It is commonly employed to enhance the strength of a wide variety of resins. Studies have shown that applying a sodium hydroxide solution to fibers significantly enhances interlocking, rises surface coarseness, and elevates hemi-cellulose weightage. Chemical treatment improves the inter-bonding characteristics of both the natural fiber and the matrix. So far, there has not been any prior

research conducted on improving the mechanical characteristics of Borassus fibers treated with alkali and reinforced with CBSSP using a statistical method called RSM. Hence, the aim of this analysis was to calculate the efficacy of alkali treatment in altering the structure, chemical properties, and thermal behavior of powdered CBSSP and Borassus fiber. Also, the analysis of the material revealed that the alkaline-treated CBSSP has the ability to improve the efficiency of natural fillers in composites, such as fibers obtained from the BF plant.

2. MATERIALS AND METHODS

2.1 CBSSP preparation

This study employed mature Caesalpinia bonducella seeds obtained from the Coimbatore district, Tamilnadu, India. The initial step involved fracturing the seed shells using a hammer.

After breaking the shells, they were thoroughly washed multiple times with filtered water to remove any impurities. The washed shells were then placed in an oven and dried at 110°C for 48 hours to eliminate any remaining moisture. Once the drying process was complete, the shells were further crushed into smaller fragments using a hammer. These crushed fragments were then ground into a fine powder using a disc-type grinding machine. The resulting seed shell powder was passed through a sieve with mesh apertures ranging from 1 to 300 µm to achieve a uniform particle size. The sieving process continued for one hour to ensure proper separation of the particles. Figure 1 illustrates the step-by-step process for the production of Biocomposite.

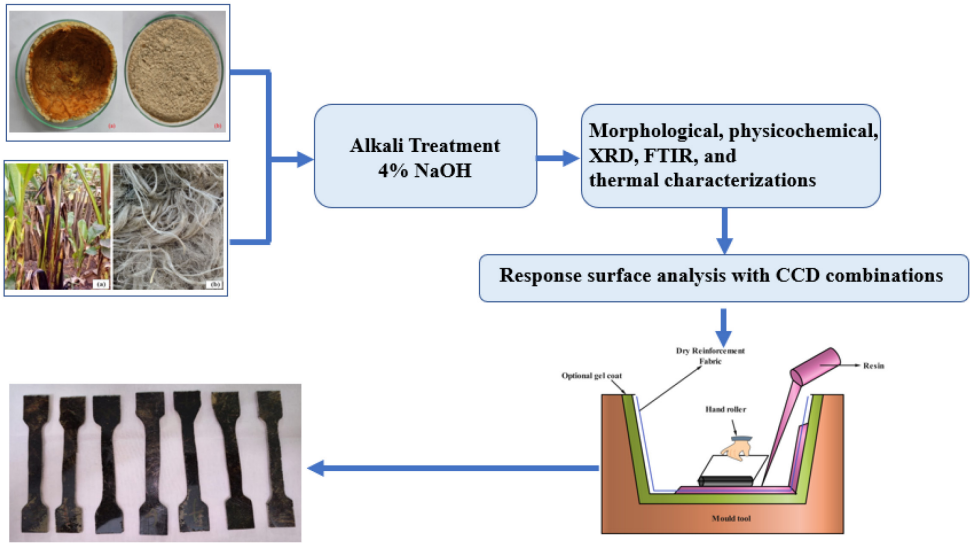

Figure 1. The diagram illustrates the sequential flow of the fabrication of bio-composites.

2.2 Surface treatment of Fiber

Subsequently, the 5% sodium hydroxide (NaOH) solution was prepared, the dehydrated specimen of CBSSP and BF were added and mixed at a speed of 150 rpm for 1 hour at ambient temperature. The specimenwas rinsed with distilled water till it attains pH (neutral) within one hour. Afterwards, it was dried for 24 hours in an oven set at 85°C.

2.3 Chemical properties

The chemical composition of the raw and NaOH-treated CBSSP specimen was analyzed, with a particular emphasis on the ratios of ash, hemicellulose, and lignin compared to cellulose. The methodologies were implemented to assess the quantities of cellulose and non-cellulose in both NaOH-treated and untreated samples. The holocellulose content of the CBSSPs (which consist of α-cellulose and hemicellulose) was determined after they were exposed to a combination of NaClO3 and NaOH solution. To ascertain the samples density, the Archimedes method was implemented.

2.4 Fourier Transform Infrared Spectroscopy

The raw and alkali-treated samples are analyzed using FTIR to identify the presence of various functional groups [33]. The palettes for FTIR analysis were prepared using a mixture that included 2 mg of the relevant sample and approximately 250 mg of potassium bromide (KBr). The containers that had been manufactured were subsequently analyzed using an FTIR spectrometer. The apparatus is configured to acquire the measurements through 32 images, each of which was conducted at a 2 cm^{-1} interval, spanning the wavenumber limits of 4000 to 400 cm^{-1}.

2.5 XRD analysis

The CI of bio-material specimen were determined using XRD analysis. The number 30 is enclosed in square brackets [30]. The radiation was quantified utilizing a powdered X-ray diffraction (XRD) instrument (D8 Bruker, ADVANCED ECO) operating at 0.02°/Sec scanning rate and covering 10-80°range. The radiation was quantified at a wavelength of 1.5406 Å (CuKα)

using an 45 kV and 25 mA. The Segal equation was employed to compute the confidence interval of the samples.

2.6 TGA analysis

Thermogravimetric analysis was performed in a nitrogen environment using a Shimadzu DTG-60 apparatus. The objective was to evaluate the thermal degradation parameters of untreated and NaOH-treated samples [34]. The temperature range examined was 30 to 600 °C, and the heating rate was set at 5 °C/min. The Shimadzu DTG-60+ instrument was employed to perform the Differential Thermal Analysis (DTA) in a N_2 atmosphere. The experiment was run at 5 °C/min, with a temperature of 30 to 600 °C. The temperature difference between the two crucibles was measured after approximately 5 mg of specimen were added to an aluminum crucible.

2.7 Morphological analysis

The raw and NaOH-treated specimen were analyzed using a SEM (ZEISS) operating at 15 kV to study their microstructural and morphological characteristics. In order to enhance the quality of the images and avoid the build-up of electrical charge, the sample were coated with a thin layer of gold sheet.

2.8 Fabrication of Borassusfiber (BF)

The high cellulose content of the fibers may lead to improved mechanical properties. Therefore, an alkali treatment has been performed to reduce the hemicellulose content. As a result, the fibers were refined from the outer layer. The retting process was used to separate the fibers from the core. Consequently, the fibers were extracted after being immersed in water to aid in their disintegration. The purified fibers were isolated from the waste material and then dried for a period of 48 hours. By thoroughly homogenizing the fibers after extraction, the impact of variance was minimized. Nevertheless, the objective of this study was to maximize the advantages of alkali treatment through the augmentation of surface roughness and improvement of mechanical properties. To produce the composites, the fibers underwent treatment with a sodium hydroxide (NaOH) solution. The specimenwas subsequently absorbed in a 5% alkali solution at ambient temperature for a duration of 24 hours, while maintaining a consistent liquid-to-fabric ratio. Following immersion in the acetic solution, the fibers were rinsed with water to cleanse them. After undergoing a 24-hour period of sun drying, they were further subjected to drying. Nevertheless, the Epoxy resin is procured from the Kovai Cheenu Enterprises, Coimbatore, Tamil Nadu, India. The epoxy resin was cured using a versatile curing agent called hexamethylenediamine.

2.9 Preparation of Composite

Subsequently, the CBSSP and processed fibers were transferred to a mold that was coated with an aerosol and had dimensions of 250 mm × 25 mm × 3 mm. Until the desired thickness was achieved, a fixed mixture of hardener and resin was progressively introduced to the fibers and CBSSP as they were layered on top of each other in order to execute a hand lay-up. The samples were subsequently subjected to a curing process in a mold at 150 °C and 2.5 MPa pressure for a duration of 5 minutes. The coupling agent utilized in this investigation was silane. Fiber-reinforced composites are frequently manufactured with the connecting agent. It improves the adhesive reactionamong the BF and epoxy matrix. The composite exhibits enhanced mechanical properties, like durability and strength, as a result of its increased adhesion. Furthermore, it exhibits enhanced resistance to environmental degradation.

2.10 RSM-based optimization of factors

The RSM technique was utilized to ascertain the optimal physical and mechanical characteristics of the BF. This required finding the optimal formulation of the fiber content (using a 10:10 ratio of BF and CBSSP), weight (20 to 30 wt.% of the composition), and fiber length (ranging from 2 to 6 mm). The present study employed RSM to ascertain the importance of independent variables, specifically the length of fiber reinforcement and the reinforcing by CBSSP. The experimental design employed the components and their respective values, as illustrated in Table 1. The tensile strength, tensile modulus, flexural strength, impact energy, and water absorption of the composite material fabricated using Epoxy, BF, and CBSSP composites were the parameters examined in this study. Table 2 presents the different parameter combinations obtained by using central composite design (CCD) to perform RSM analysis. [35].

Table1: Input parameters and its levels.

Factors	Symbol	Levels		
		-1	0	+1
BF + CBSSP mixture (wt%)	A	20	25	30
Length of Fibre (mm)	B	2	4	6

Table 2: Factors combinations using CCD.

S. No	Weight of BF + CBSSP (1:1)(% wt)	Length of the Fiber (mm)
1	25	2
2	20	4
3	20	2
4	25	4
5	30	6
6	30	2
7	20	6
8	30	4
9	25	6

In order to ascertain the optimal values for water absorption, tensile strength, flexural strength, tensile modulus, and impact energy, this investigation implemented the Response Surface Methodology (RSM) in conjunction with the central composite

design (CCD). The central composite design (CCD) was implemented at all three levels, as indicated in Table 2, for each of the independent parameters: fibre weight, CBSSP weight, and fibre length. The coded values (-1, 0, and 1) were used for each parameter. To understand the impact of each chosen independent variable and their interactions on the selected responses, it is necessary to examine the outturn. Equation (1) is a linear formula that expresses the correlation among the response and the independent variables.

$$P_i = b_o + b_1X_1 + b_2X_2 + b_{12}X_1X_2 \ldots\ldots. (1)$$

Pi is a response variable that is distinct for i values between 2 and 6. The value of b0 remains unchanged. The variables b1 and b2 denote the linear coefficients, whereas b12 denotes the coefficient for interaction. The independent variables, biomaterial weight (BF and CBSSP s) and fiber length were set to vary from 20 to 30 wt. % and 2 to 6 mm, respectively.

2.11 Fabrication of biocomposite

In this study, bio-composite plate samples were formed using a stainless-steel mold with dimensions of 280 × 200 × 5 mm. A base plate and a detachable mount are the two components of the mold, which facilitate the effortless removal of the composite. Following the creation of the mold, wax was covered uniformly to all of its surfaces. To expedite the release of the composite, a consistent layer of wax is applied to all internal surfaces of the mold.

2.12 Analysis of mechanical properties

The tensile testing of the specimens, which were 250 × 25 mm and characterized by a dumbbell shape, was carried out in accord with the ASTM D-638-03 criteria. Tensile force was applied at a rate of 2 mm/min to conduct the experiments. A flexural test was conducted in accord with the criteria specified in ASTM D790, utilizing a Universal testing Machine (FIE, India, F150 series). The experiment employed a specimen with dimensions of 250 mm in length, 25 mm in width, and 3 mm in thickness. The Izod impact test was conducted in accordance with the specifications defined in ASTM D256-10. This impact analysis utilized a rectangular object with dimensions of 127 x 10 x 3mm^3 in height with a velocity of 1.5 m/s at an angle of 60°.

2.13 Analysis of physical property

The physical properties of fiber-reinforced epoxy can be compromised by matrix fractures, water absorption, and dimensional instability. The water absorption properties of the composites were assessed in accordance with the ASTM D 570 standard. Initially, the specimens were assessed for their mass using a precise weighing instrument. As a result, this mass was employed as the initial for moisture absorption test. Additionally, the weights of the samples were ascertained subsequent to their immersion in water. The water absorption was determined by the composite's ultimate mass. Over the duration of one week, a water absorption test was conducted for 168 hours. The composites were weighed after filter paper was used to capture any residual water. Equation (2) was implemented to determine the materials' water absorption percentage.

$$Moisture\ Content = \frac{M_2 - M_1}{M_1} \times 100 \quad (2)$$

Let M_1 represent the primary weight of the specimen and M_2 represent the final weight of the specimen after immersion.

2.14 Statistical analysis

A precise two-dimensional surface diagram was constructed using the Design Expert software to examine the relationship between a response and two variables. The model term is deemed important if p-value < 0.05 in order to establish statistical sufficiency.

3. RESULTS AND DISCUSSIONS

3.1 SEM analysis

Figure 2(a) and 2(b) depict the morphology of the untreated and alkali-treated EV fiber, respectively, as observed under a scanning electron microscope (SEM). Figure 3(a) and 3(b) display the scanning electron microscopy (SEM) images of untreated and NaOH-treated CBSSP's correspondingly.

3.2 Density and chemical properties

In contrast to untreated CBSSPs, alkali-treated CBSSPs exhibited a higher cellulose content. Table 3 displays the density and chemical composition of Caesalpinia bonducella shell powder. The research revealed that the levels of hemicellulose, lignin, and ash in CBSSP that had been treated with alkali had decreased. Additionally, these particles established robust and enduring connections with the matrix when they were employed as reinforcement in polymer matrix composites (PMC).

The primary factor contributing to the increased density of modified CBSSPs is the removal of non-cellulosic components from the particles during the alkalization process. The removal process can generate vacancies that particles can use to retain molecules. Table 1 displays the chemical composition of untreated and alkali-treated CBSSP.

3.3 FTIR analysis

The distinct functions of the infrared (IR) peaks of both untreated and alkaline-treated CBSSP samples are illustrated in Figure 4. The wide absorption band extending from 3200 to 3500 cm −1 indicates that the O-H bond in CBSSP treated with NaOH was less prominent, as reflected in the results. The OH groups in fatty acids tend to consolidate when they interact with the carboxylic bonds of CBSSP. The C-H bond's elongation is indicated by the occurrence of a peak at 2897.51 cm^{-1}. Nevertheless, the peak shifted to 2884.12 cm^{-1} as a consequence of the significant extraction of hemicellulose from the particles treated with NaOH. Raw CBSSP samples exhibits an absorbing band with a peak at 1744.82 cm^{-1}, which is indicative of the occurrence of the carbonyl group C = O. However, after applying alkali treatment, this band dissolved entirely because hemicellulose underwent hydrolysis, causing the C-O-C

linkages among the two monomers to break. The chemically treated CBSSPs exhibited substantial removal of lignin and hemicelluloses, as evidenced by the lack of this peak.

The raw CBSSPs exhibit a peak intensity at 1241.74 cm^{-1}, which is indicative of the modulation of hemicellulose (-COO) and the elongation of lignin (C-O). The absence of this peak in the treated CBSSPs provides further evidence that the alkali treatment has effectively removed hemicellulose and lignin from the surface of the CBSSPs. The evidence that the hemicellulose and lignin components have been eradicated from the surface of the CB shell particle following chemical treatment is provided by the observation of a diminished peak at 1017.65 cm^{-1}.

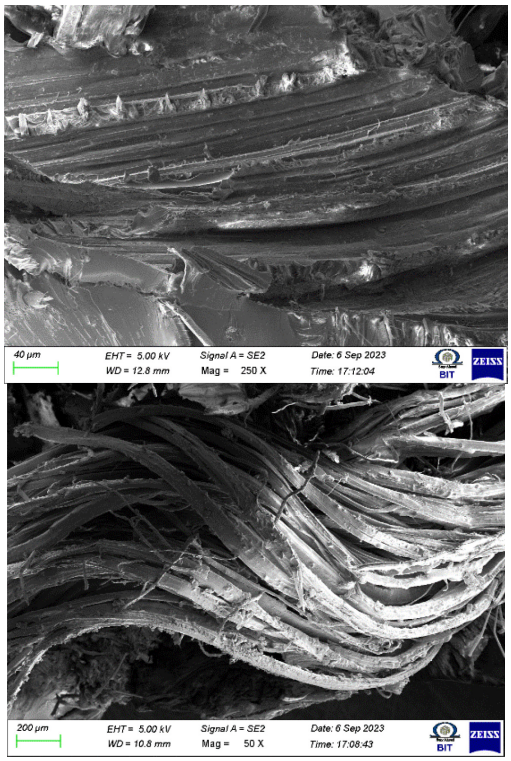

Figure 2. SEM image of (a) untreated and (b) alkali-treated BF

Table 3. Density and Chemical composition of CBSSP.

CBSSP s	Density (g/cm^3)	Lignin (wt %)	Hemicellulose (wt%)	a-Cellulose (wt%)	Ash (wt %)
Untreated	1.22	28.5	22.3	44.8	4.4
Alkali-treated	1.25	22.0	18.7	53.0	3.2

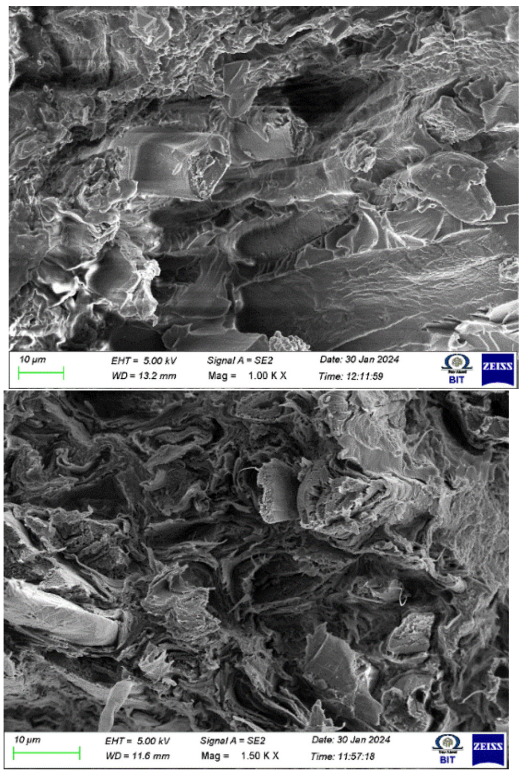

Figure 3 SEM image of (a) untreated and (b) NaOH-treated CBSSP s.

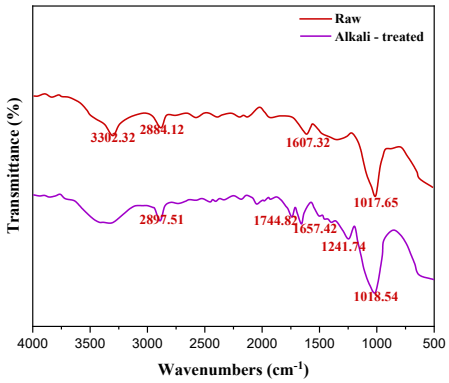

Figure 4. Evaluation of FTIR spectrum obtained from raw and alkali-treated CBSSP

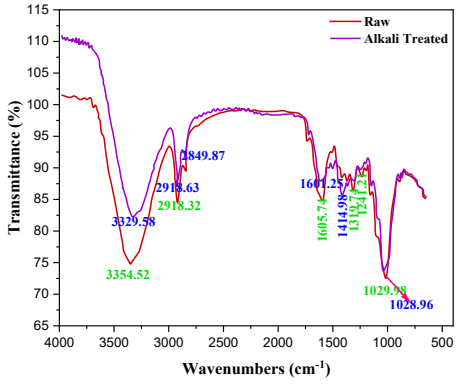

Figure 5. Evaluation of FTIR spectrum for raw and alkali-treated BF

Figure 5 demonstrates the study of the FTIR spectra of untreated BF and BF that has been treated with alkali (ABF). The principal functional groups present in the fibers were identified through the examination of the spectra. The results suggested that the significant peak observed at 3329.58 cm^{-1} was caused by the elongation of OH bonds, which is evidenced by the presence of cellulose. The stretch vibration of the C-H bonds, which is induced by the occurrence of cellulose constituent's C-H groups is the cause of the peak observed at 2918.63 cm^{-1}. Furthermore, a minor absorption signal at 2849.87 cm^{-1} was used to identify the C-H symmetricalwinding of the NaOH group. In addition to an additional peak, the ABF compound exhibited stretching vibrations of the carbonyl functional group at frequencies of 161.25 cm^{-1} and 1414.98 cm^{-1}. The presence of an alkyl halide functional group results in the detection of a distinctive peak at 1033 cm^{-1}. The existence of biological constituents is corroborated by the presence of peaks in the FTIR spectra, as asserted by ABF.

3.4 XRD analysis

The XRD spectra of the untreated and alkali-treated CBSSP samples are depicted in Figure 6. The intensity observed at an angle of 20.14° (2θ) was used to confirm the presence of the amorphous phase. On the other hand, the cellulose-I phase was identified by the peaks that were observed at angles of 16.58°, 18.51°, 23.12°, and 35.85°. These angles correspond to the crystallographic planes 120, 140, 210, and 005, correspondingly. Nevertheless, the contaminants present in the CBSSP samples were the cause of the residual XRD peaks. Equation (3) has been employed to ascertain the Crystallinity Index (CI) of the CBSSP particles. The CI value increased significantly from 41.74% in the original sample to 54.08% as a consequence of the applied alkali treatment to CBSSP, which removed the disordered components. Equation (4) was implemented to ascertain the crystallite size (CS) of the CBSSP. In comparison to untreated CBSSPs, alkali-treated CBSSPs exhibited a higher CS of 12.34 nm and a lower CS of 8.79 nm. The CBSSP materials exhibit enhanced chemical reactivity and moisture resistance as the concentration of the CS component increases. Consequently, while amorphous compounds can be produced from CBSSPs, granules are more effective when used as strengthening in matrix composites.

$$CI = \frac{I_{200} - I_{AM}}{I_{200}} \times 100 \quad (3)$$

The CS was calculated using Scherrer's equation, which utilizes the highest CI phase (I200) at an angle of 2θ = 23 - 25°, and the intensity of the amorphous phase (IAM) at an angle of 2θ = 20 - 22°.

$$CS = \frac{k\lambda}{\beta cos\theta} \quad (4)$$

The variables used in this context are: K, which represents Scherrer's constant with a value of 0.89; β, which stands for FWHM; and λ, which represents the wavelength of the radiation with a value of 0.1541 nm.

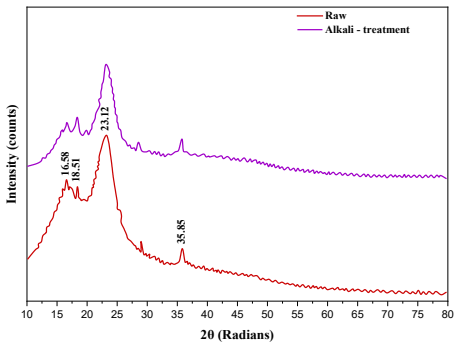

Figure 6. The XRD spectrum of untreated and NaOH-treated CBSSP

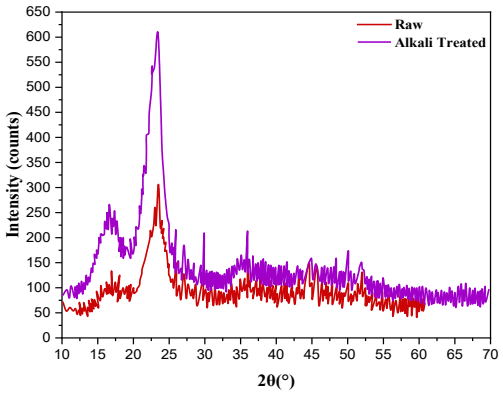

Figure 7. Evaluation of XRD spectrum for untreated and NaOH treated with alkali BF.

Figure 7 displays the XRD patterns of the pure ethylene-vinyl fluoride (EVF) and pure alternating ethylene-vinyl fluoride (AEVF) samples. The data exhibit two distinct peaks, observed at 2Θ = 16.73° and 2Θ = 23.58°, which are easily discernible. The underlying semi-crystalline nature of the ABFF was evident from these two peaks. Based on the findings, it was determined that AEVF exhibited an amorphous structure due to the presence of the (1 1 0), which was accountable for the initial peak at 16.73°. (Iam). The existence of a secondary peak at an angle of 23.58°, which aligned with the (2 0 0) crystallographic plane, suggests that the fiber possessed a crystalline structure. The residual weak spectral peaks indicated the existence of contaminants in AEVF.

3.5 TGA analysis

Evaluating the thermal properties of CBSSPs is crucial in determining their suitability as reinforcing fillers in bio-composites[36]. The process of thermal deterioration for both untreated particles and alkali-treated CBSSPs is depicted in Figure 8. The sample is primarily subjected to thermal degradation in three distinct phases. It was discovered that the early degradation temperatures of untreated CBSSP ranged from 60 to 200°C, whereas those of alkali-treated CBSSP were 90 to 220°C. Withdrawal of moisture from CBSSPs during deterioration is a hallmark of this temperature range. CBSSP and the treated CBSSP samples saw a weight decrease of approximately 10-13% within this specific temperature range.

The second degradation temperature of untreated CBSSP varied from 200 to 350 °C, whereas for CBSSP treated with alkali, it ranged from 240 to 380 °C. Within this temperature range, the decomposition of lignin and hemicellulose, which are parts of CBSSPs, takes place. The untreated CBSSP samples experienced a weight reduction of approximately 58.48% within a certain temperature range, while the CBSSP samples treated with alkali displayed a weight reduction of 62.48%. The degradation temperature of both untreated and alkali-treated CBSSPs was found to range from 350 to 500 °C, indicating the decomposition of lignin and cellulose. Lignin degradation persists until it reaches temperatures of 600°C. Figure 9 depicts the thermal efficiency of ABF and BF. The decrease in weight of the fiber commenced at a temperature of 82.18°C, which can be ascribed to the decrease in moisture content. Another slight reduction in weight was seen at approximately 160 °C, which was ascribed to the breakdown of lignin. The thermal steadiness of ABF was evaluated to be approximately 260 °C. Though, a following decline in quality, associated with the breakdown of hemicelluloses through heat depolymerization, was observed between temperatures of 260 °C and 370 °C.

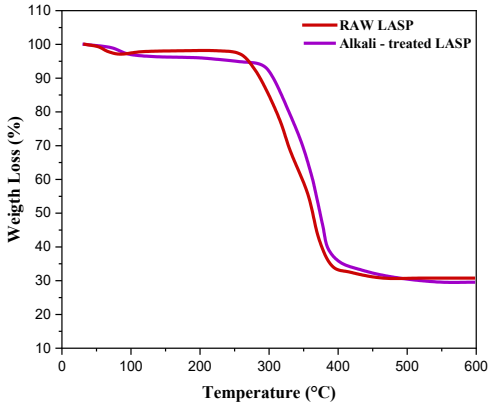

Figure 8. Comparison of weight loss in TGA analysis for untreated CBSSP s and alkali-treated CBSSP.

3.6 Utilizing Response Surface Methodology (RSM) to conduct compositional study of the properties of the bio-composite

The distribution of reinforcement weight in a polymer-fiber composite quickly changes its physio-mechanical characteristics. Adding more fiber reinforcement increases most physio-mechanical parameters except water absorption capacity. Table 4 shows the obtained results for different parameter mixturesby utilizingCentral composite design. The length of the reinforcing fibers is a crucial factor in defining the mechanical and physical properties of polymer matrix-fiber composites. The only more important component is the weight composition of the fibers, however this is the second most important factor. According to studies, longer fiber reinforcements often have better physio-mechanical characteristics. However, it has been demonstrated that physiochemical characteristics tend to decrease after a specific length is attained, which is contingent upon the fiber type.

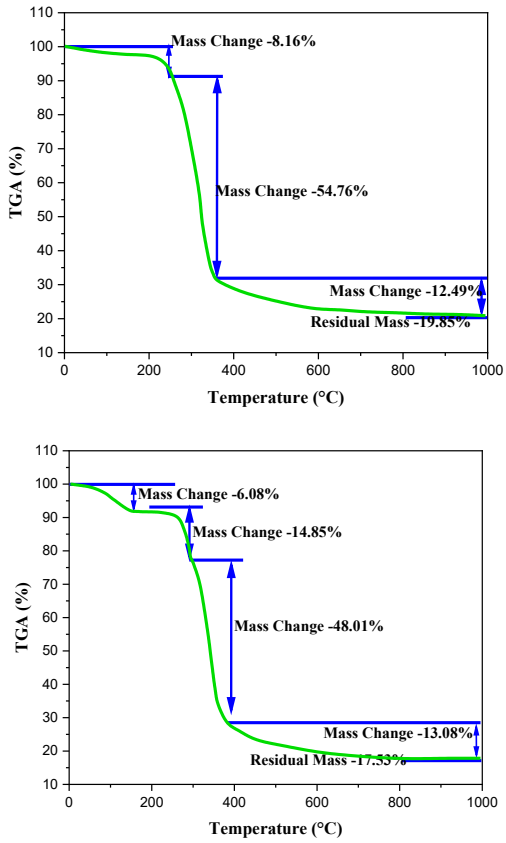

Figure 9. The thermal degradation performance of (a) BF and (b) ABF.

Table 5 displays the RSM models that were created for the epoxy-Borassus fiber composite based on the response parameters that were actually used. Table 6 are the findings from the trials concerning water absorption, tensile modulus, and modified R^2. A regression model's sufficiency can be evaluated using the modified R^2 test. ANOVA was employed to assess the correctness of coefficients for the quadratic polynomial equations. The importance of each phrase is indicated by its elevated F-value and comparatively low P-value.

The most influential elements that determined the linear connection between biomaterial loading and fiber reinforcement length were those related to tensile modulus ($P \leq 0.05$). The parameters that influenced the tensile strength had a far greater impact than the individual impacts of the reinforcing weight and fiber length of the biomaterials ($P \leq 0.05$). Furthermore, the linear relationship between the length of fibers and the loading of biomaterial and the individual impact of the weight of fiber reinforcement, also had a significant impact. There was a range of extremely significant to marginally significant degrees of influence on water absorption ($P < 0.05$). Furthermore, the model's appropriateness in accurately forecasting the experimental results is compellingly demonstrated by the high values of R^2 and modified R^2. These findings confirm that the linear model is suitable for the data in light of the particular experimental conditions[37]. However, the corrected R^2 values were comparatively low, indicating that there were discrepancies between the observed and predicted tensile modulus results.

Table 4. Obtained responses for design of experiments.

Std	Run	TS	TM	FS	IE	Moisture Absorption
7	1	11.21	263	15.92	0.819	0.349
3	2	12.11	230	20.67	0.76	0.218
9	3	10.78	353	14.31	0.67	0.201
2	4	11.41	253	24.8	0.843	0.366
5	5	16.07	275	28.28	0.97	0.577
8	6	10.54	255	26.72	0.95	0.365
6	7	10.48	207	27.02	0.858	0.24
4	8	13.18	257	25.58	0.959	0.443
1	9	12.91	235	27.68	0.907	0.379

Figure 10. The samples of a composite material made from epoxy resin, Borassus fiber and CBSSP

Table 5. RSM models for epoxy-BF fiber composite's selected response properties

Response	RSM Model
Tensile Strength	= 18.992 - 0.369 A - 3.066 B + 0.14575 A * B
Tensile Modulus	= 727.5 - 16.7 A - 116.58 B + 4.15 A * B
Flexural Strength	= -28.593 + 1.734 A + 9.138 B - 0.2787 A * B
Impact Energy	= - 0.1516 + 0.0365 A + 0.1297 B - 0.0042 A * B
Water Absorption	= 0.0825 + 0.0069 A - 0.0847 B + 0.004325 A * B

Table 6. ANOVA tablefor the hybrid composite.

Source	Sum of Squares	df	Mean Square	F-value	p-value	
Tensile Strength						
Model	23.37	3	7.79	17.11	0.0046	significant
A-A	6.87	1	6.87	15.09	0.0116	
B-B	8.00	1	8.00	17.58	0.0085	
AB	8.50	1	8.50	18.66	0.0076	
Residual	2.28	5	0.4553			
Cor Total	25.65	8				
R^2	0.9112		Adj.R^2	0.8580		
Tensile Modulus						
Model	10843.17	3	3614.39	7.40	0.0275	significant
A-A	1.50	1	1.50	0.0031	0.9579	
B-B	3952.67	1	3952.67	8.10	0.0360	
AB	6889.00	1	6889.00	14.11	0.0132	
Residual	2440.83	5	488.17			
Cor Total	13284.00	8				
R^2	0.8163		Adj.R^2	0.7060		
Flexural Strength						
Model	201.54	3	67.18	19.26	0.0035	significant
A-A	57.54	1	57.54	16.49	0.0097	
B-B	112.93	1	112.93	32.37	0.0023	
AB	31.08	1	31.08	8.91	0.0306	
Residual	17.44	5	3.49			

Cor Total	218.99	8				
R^2	0.9203		Adj.R^2	0.8725		
Impact Energy						
Model	0.0799	3	0.0266	324.64	< 0.0001	significant
A-A	0.0582	1	0.0582	709.82	< 0.0001	
B-B	0.0146	1	0.0146	178.06	< 0.0001	
AB	0.0071	1	0.0071	86.04	0.0002	
Residual	0.0004	5	0.0001			
Cor Total	0.0803	8				
R^2	0.9949		Adj.R^2	0.9918		
Water Absorption						
Model	0.1085	3	0.0362	38.30	0.0007	significant
A-A	0.0878	1	0.0878	93.03	0.0002	
B-B	0.0132	1	0.0132	13.94	0.0135	
AB	0.0075	1	0.0075	7.92	0.0373	
Residual	0.0047	5	0.0009			
Cor Total	0.1132	8				
R^2	0.9583		Adj.R^2	0.9333		

The regression analysis results for the first-degree polynomial model and the data for TM, water absorption, and other variables, are presented in Table 6. The findings indicated that the impact energy and flexural strength were enhanced by increasing the quantity and size of fiber reinforcement. Conversely, the tensile strength and tensile modulus were both enhanced as a consequence of a decrease in the quantity and size of fiber reinforcement. Nevertheless, the biomaterials' water absorption increased as a result of their improved quality and reduced size. In general, RSM employed to examine the effects of biomaterial composition and fiber length on water absorption, TM, and TS, both individually and in conjunction. Therefore, the Epoxy and Borassus fiber composite was improved by using CCD and RSM techniques, leading to positive results. The independent variables' reactions are the source of the experimental data. Based on the study and analysis that followed, it is possible to use reaction surface plots and the linear polynomial equation to determine the water absorption and tensile modulus.

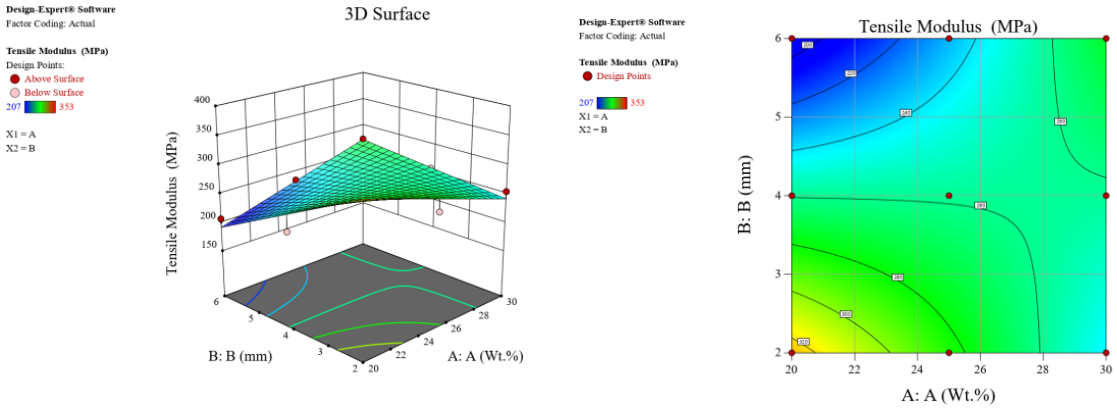

Figure 11. Response plots for tensile modulus

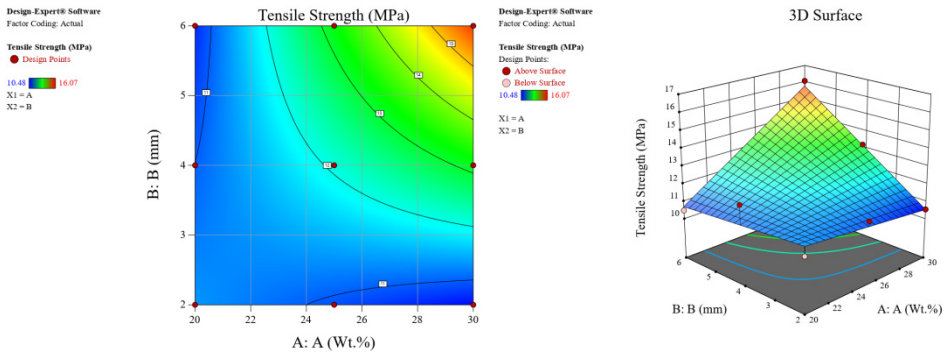

Figure 12. RSM plots for tensile strength

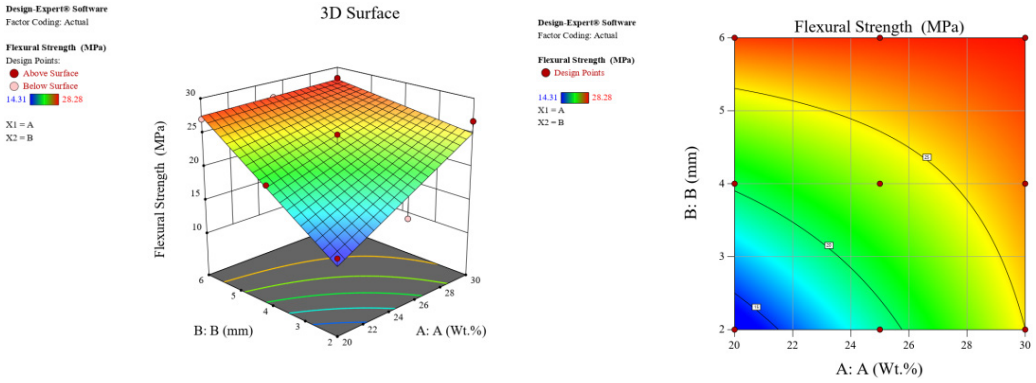

Figure 13. RSM plots for flexural strength

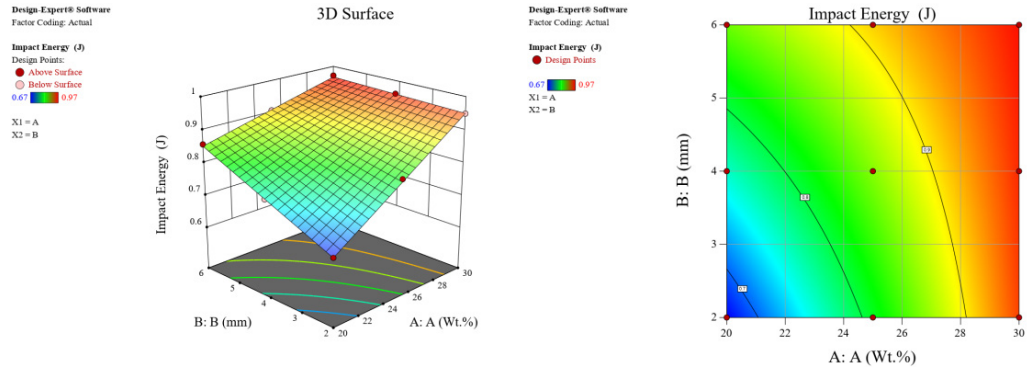

Figure 14. RSM plots for impact energy

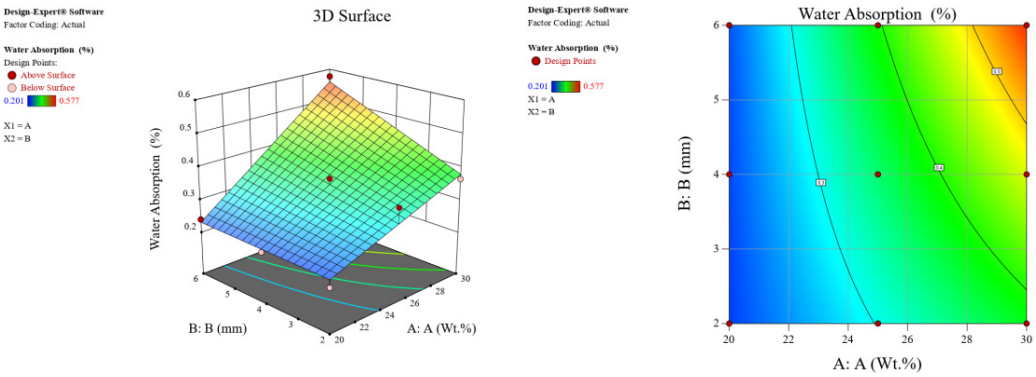

Figure 15. RSM plots for water absorption

The RSM-generated contour and response surface diagrams for the tensile modulus, water absorption, impact energy, and flexural strength variables are shown in Figure 11-15. The independent factors have a considerable impact on the composite material's qualities when made with Borassus fiber and epoxy. Analysis of the fiber characteristics of the composite material yielded a tensile modulus of 275 MPa. Researchers found that reducing the reinforcing fibers' weight, composition, and length enhanced their tensile modulus. Composite materialsshowed a minimum tensile strength of 10.48 MPa, as shown by the effect of fiber properties on this property. The tensile modulus is typically found to rise in direct proportion to the reinforcing fibers' weight and length. Figure 13 shows a surface plot of the independent parameters affecting the three-dimensional flexural strength of the Epoxy-fiber composite. By investigating the impact of fiber properties, the composite achieved a minimum flexural strength of 14.31 MPa. The weight of the fiber reinforcement typically has a minimal impact. However, research has demonstrated that the flexural strength is improved by elongating the fibers. Figure 14 illustrates the correlation between fiber properties and impact energy, indicating that the composite material attained a minimum impact energy of 0.67 J.

The impact energy appears to have risen in proportion to the increase in weight of the reinforcing fibers, and their length and composition. Compared to the findings obtained for various fibers, this particular one exhibited consistency. Figure 15 illustrates the two-dimensional response surface of water absorption in an epoxy-Borassus fibre composite. The composite exhibited the lowest water absorption rate of 0.201%, as determined by the analysis of the fiber characteristics. Fiber

reinforcements possessing reduced weight, composition, and length exhibited diminished water absorption. Consistent with previous research on various types of fibers, this study observed that the water absorption of natural fibers increases as their length and weight composition increase. This occurs due to an increase in the quantity of unbound hydroxyl (-OH) groups inside the fiber, resulting in a larger concentration of cellulose. Consequently, the fiber's capacity to absorb water is enhanced. The aforementioned properties were optimized using numerical optimization models to create the ideal Epoxy-Borassus fiber composite. This composite has a limited capacity to absorb water, a high resistance to deformation under tension, and strong resistance to bending and impact when it is reinforced with 4 mm long fibers and 25% by weight of biomaterials.

4. CONCLUSION

This study explores the capacity of Borassus fibers, an underused biomaterial, in the advancement of Epoxy-BF fiber composites. The study used Caesalpinia bonducella seed shell powder (CBSSP) particles as a strengthening agent. The biomaterials were subjected to NaOH treatment, which led to substantial enhancements in their compatibility, as evidenced by the microstructural, physico-chemical, FTIR, XRD, and thermal analyses. The Response Surface Methodology based Central Composite Design was employed to evaluate the characteristics of the Epoxy-BF composite. Consequently, the TM, TS, FS, IE, and moisture absorption of the composite were enhanced by modifying the length and quantity of fibers in alkali-treated biomaterials. Polynomial equations of the first degree were devised to investigate the composite material's properties in relation to the fiber length and biomaterial loading. The composite material's tensile modulus was determined to be 275 MPa through the analysis of the fiber properties. The composite attained a minimum flexural strength of 14.31 MPa after an analysis of the impact of fiber characteristics. Additionally, the properties of the fibers were demonstrated to influence the water absorption of the composite material. The composite demonstrated the lowest absorption rate, surpassing other materials by a margin of 0.201%. The composite properties were optimized through the use of numerical models to generate the optimal Epoxy-Borassus fiber composite. This composite demonstrates the tensile modulus, impact energy, flexural strength, and low water absorption. By incorporating a 4 mm fiber length reinforcement with a 25 wt % addition of biomaterials reinforcement, these qualities were achieved.

REFERENCES

[1] B. Mahendiran, S. Muthusamy, S. Sampath, S. N. Jaisankar, R. Selvakumar, and G. S. Krishnakumar, “In vitro and in vivo biocompatibility of decellularized cellulose scaffolds functionalized with chitosan and platelet rich plasma for tissue engineering applications,” Int J Biol Macromol, vol. 217, pp. 522–535, 2022. DOI:/10.1016/j.ijbiomac.2022.07.052

[2] B. Mahendiran, S. Muthusamy, G. Janani, B. B. Mandal, S. Rajendran, and G. S. Krishnakumar, “Surface Modification of Decellularized Natural Cellulose Scaffolds with Organosilanes for Bone Tissue Regeneration,” ACS Biomater Sci Eng, vol. 8, no. 5, pp. 2000–2015, 2022. DOI:10.1021/acsbiomaterials.1c01502

[3] S. K. Sharma and B. U. Kelkar, “Effect of densification on certain physical and mechanical properties of inner soft wood of Borassus flabellifer L.,” Journal of the Indian Academy of Wood Science, vol. 18, no. 1, pp. 39–44, 2021. DOI:10.1007/s13196-021-00277-1

[4] S. Rai P., H. N., K. D.V., S. Unnikrishnan, and C. A., “Mechanical strength and water penetration depth of palmyra fibre reinforced concrete,” in Materials Today: Proceedings, 2022, pp. 1881–1886. DOI:10.1016/j.matpr.2022.05.049

[5] R. S. Akshana, N. Sobini, T. Kirushanthi, and S. Srivijeindran, “Synthesis of Cellulose Nano Fiber from Palmyrah Fruit Fiber and its Applicability as a Reinforcement Agent on Starch Based Biodegradable Film,” Ceylon Journal of Science, vol. 53, no. 3, pp. 313–320, 2024. DOI:10.4038/cjs.v53i3.8257

[6] M. N. Abubakar, T. K. Bello, M. T. Isa, and K. Lawal, “Effect of alkaline treatment on the physical and mechanical properties of borassus flabellifer leaf fiber,” Polymer Bulletin, vol. 80, no. 12, pp. 12577–12590, 2023. DOI:10.1007/s00289-022-04666-5

[7] M. J. Mukkadan, R. Preetha, and V. Sreejit, “Development of active packaging film reinforced with nano cellulose extracted from Palmyra palm (Borassus flabellifer) residues for prolonging the shelf life of chicken meat,” Int J Food Sci Technol, vol. 59, no. 3, pp. 2033–2041. DOI:10.1111/ijfs.16706

[8] S. Sakib et al., “Effect of fibre orientation and stacking sequence on properties of hybrid composites,” Materials Science and Technology (United Kingdom), vol. 39, no. 13, pp. 1627–1639, 2023. DOI:10.1080/02670836.2023.2177803

[9] K. T. Kumar, R. Sudhakaran, and A. V Murugan, “Sulfonate Functionalized Turbostratic Carbon Derived from Borassus flabellifer Flower: A Ultrathin Protective Layer to Mitigate the Dendrite Formation on the Metallic Lithium Anode,” ACS Sustain Chem Eng, vol. 10, no. 43, pp. 14151–14162, 2022. DOI:10.1021/acssuschemeng.2c03212

[10] J. K. Singh and A. K. Rout, “Study on the physical, mechanical, and thermal behaviour of RHN blend epoxy hybrid composites reinforced by Borassus flabellifer L. fibers,” Cellulose, vol. 30, no. 8, pp. 5033–5049, 2023. DOI:10.1007/s10570-023-05191-y

[11] J. K. Singh and A. K. Rout, “Experimental investigation on tribo-performance of rice husk nanoparticles blend epoxy composites reinforced by Borassus flabellifer L. fibre using neural network approach,” Mater Today Commun, vol. 38, 2024. DOI:10.1016/j.mtcomm.2023.107971

[12] V. Vadivelvivek, N. Natarajan, K. Nijandhan, and C. Boopathi, “INVESTIGATION OF MECHANICAL PERFORMANCE OF BORASSUS FLABELLIFER SPROUT FIBER REINFORCED POLYMER COMPOSITES,” Cellulose Chemistry and Technology,

vol. 57, no. 5–6, pp. 637–644, 2023. DOI:10.35812/CelluloseChemTechnol.2023.57.58

[13] K. Dash, J. Nanda, S. N. Das, and V. C. Jha, "Compressive characterization of different chemically treated Borassus flabellifer fruit fibers," SPE Polymers, vol. 5, no. 2, pp. 127–135, 2024. DOI:10.1002/pls2.10107

[14] N. P. Sunesh, S. Indran, D. Divya, and S. Suchart, "Isolation and characterization of novel agrowaste-based cellulosic micro fillers from Borassus flabellifer flower for polymer composite reinforcement," Polym Compos, vol. 43, no. 9, pp. 6476–6488, 2022. DOI:10.1002/pc.26960

[15] J. K. Singh, A. K. Rout, and K. Kumari, "A review on Borassus flabellifer lignocellulose fiber reinforced polymer composites," CarbohydrPolym, vol. 262, 2021. DOI:10.1016/j.carbpol.2021.117929

[16] S. S. Kumar, I. P. Sudagar, P. Rajkumar, R. Naik, and R. Kavitha, "Selected engineering properties of palmyrah (Borassus flabellifer) leaf base," Journal of Plantation Crops, vol. 49, no. 3, pp. 200–213, 2021. DOI:10.25081/jpc.2021.v49.i3.7454

[17] A. Chakraborty, P. Ghalsasi, and P. Radha, "Green Engineering: Poly (lactic acid) Composite Materials Fortified with Surface-Modified Nanocellulose from Borassus flabellifer Leaves," Biomass Convers Biorefin, 2024. DOI:10.1007/s13399-024-05670-7

[18] V. Balasubramani, K. J. Nagarajan, M. Karthic, and R. Pandiyarajan, "Extraction of lignocellulosic fiber and cellulose microfibrils from agro waste-palmyra fruit peduncle: Water retting, chlorine-free chemical treatments, physio-chemical, morphological, and thermal characterization," Int J Biol Macromol, vol. 259, 2024. DOI:10.1016/j.ijbiomac.2024.129273

[19] T. Ganesan, N. Jayarajan, and D. Ramachandran, "Investigating the impact of epoxy Borassus flabellifer fiber-based composites for UAV landing gear," Iranian Polymer Journal (English Edition), 2024. DOI:10.1007/s13726-024-01323-8

[20] P. Khamkat, B. Chatterjee, V. Barik, D. Patra, and A. Chakraborty, "Extraction, Characterization and Antibacterial Potential Assessment of Polar Phytoconstituents of Caesalpinia bonducella Seeds Extract," YuzuncuYil University Journal of Agricultural Sciences, vol. 34, no. 1, pp. 115–127, 2024. DOI:10.29133/yyutbd.1362736

[21] D. Singh Maravi, P. Dixit, A. K. Dixit, and R. K. Vandre, "Comparative efficacy of crude seed powders of caesalpiniabonducella, butea monosperma and moringa oleifera against benzimidazole susceptible gastrointestinal nematodes of goats," Journal of Veterinary Parasitology, vol. 37, no. 1, pp. 55–59, 2023. DOI:10.5958/0974-0813.2023.00008.6

[22] S. Mathiyazhagan, H. Yadav, R. Vishwanathan, and A. Reddy, "Finding the Principle Leads using GC-MS and Unravelling the Anti-inflammatory Activity of Alkaloid Isolated from Caesalpinia bonducella by in vitro Techniques," Indian Journal of Pharmaceutical Education and Research, vol. 57, no. 2, pp. s345–s352, 2023. DOI:10.5530/ijper.57.2s.40

[23] S. Nithiyanandam, V. Jaisankar, M. Parthasarathy, R. Katturajan, and S. E. Prince, "Antioxidant mediated defensive potency of Caesalpinia bonducella nut on Acetaminophen-inebriated spleen and cardiotoxicity: Implications on oxidative stress and tissue morphology in an In vivo model," Indian J BiochemBiophys, vol. 60, no. 4, pp. 297–306, 2023. DOI:10.56042/ijbb.v60i4.72352

[24] P. Ezhilarasan, S. Sivakrishnan, and S. Vigil Anbiah, "Phytochemical analysis of ethanolic extract of leaves of Caesalpinia bonducella," Res J Pharm Technol, vol. 14, no. 11, pp. 5891–5894, 2021. DOI:10.52711/0974-360X.2021.01024

[25] B. Gaddalaet al., "Exploring the impact of hybridization on green composites: Pineapple leaf and sisal fiber reinforcement using poly(furfuryl alcohol) bioresin," Zeitschrift fur PhysikalischeChemie, 2024. DOI:10.1515/zpch-2024-0772

[26] T. Bothiraj, K. Boopathi, K. Kalaiselvan, A. Benham, and S. Mayakannan, "Experimental investigations on mechanical and wear behavior of waste marble dust and coconut fiber reinforced hybrid bio composites," in Materials Today: Proceedings, Elsevier Ltd, 2022, pp. 2239–2242. DOI:10.1016/j.matpr.2022.08.441

[27] S. Thangaraj, G. M. Pradeep, M. S. Heaven Dani, S. Mayakannan, and A. Benham, "Experimental investigations on tensile and compressive properties of nano alumina and arecanut shell powder reinforced polypropylene hybrid composites," in Materials Today: Proceedings, Elsevier Ltd, 2022, pp. 2243–2248. DOI:10.1016/j.matpr.2022.08.442

[28] R. Jayaraman, R. Girimurugan, V. Suresh, C. Shilaja, and S. Mayakannan, "Improvement on Tensile Properties of Epoxy Resin Matrix Sugarcane Fiber and Tamarind Seed Powder Reinforced Hybrid Bio-Composites," in ECS Transactions, Institute of Physics, 2022, pp. 7265–7272. DOI:10.1149/10701.7265ecst

[29] R. Girimurugan, G. B. Loganathan, G. Sivaraman, C. Shilaja, and S. Mayakannan, "Compressive Behavior of Tamarind Shell Powder and Fine Granite Particles Reinforced Epoxy Matrix Based Hybrid Bio-Composites," in ECS Transactions, Institute of Physics, 2022, pp. 7111–7118. DOI:10.1149/10701.7111ecst

[30] R. Girimurugan, C. Shilaja, S. Mayakannan, S. Rajesh, and B. Aravinth, "Experimental investigations on flexural and compressive properties of epoxy resin matrix sugarcane fiber and tamarind seed powder reinforced bio-composites," in Materials Today: Proceedings, Elsevier Ltd, 2022, pp. 822–828. DOI:10.1016/j.matpr.2022.04.386

[31] P. Ghalsasi, P. M. Rao, S. Sruthi, V. S. Avanthi, and P. Radha, "Unveiling the Potential of Borassus flabellifer's Leaves Derived ZnO Nanoparticles in Augmenting the Attributes of PLA-Surface Modified Nanocellulose Bio-composite," J Polym Environ, 2024. DOI:10.1007/s10924-024-03220-w

[32] B. NagarajaGanesh, B. Rekha, C. Kailasanathan, P. Ganeshan, and V. Mohanavel, "Sustainable fiber extraction and determination of mechanical and wear properties of Borassus flabellifer sprout fiber-reinforced polymer

composites," Biomass Convers Biorefin, 2024. DOI:10.1007/s13399-024-05480-x

[33] A. G. Adeniyi et al., "Mechanical and microstructural properties of expanded polyethylene powder/mica filled hybrid polystyrene composites," Mechanics of Advanced Materials and Structures, vol. 30, no. 13, pp. 2610–2619, Jul. 2023, DOI: 10.1080/15376494.2022.2059822.

[34] S. A. El-Sayed, T. M. Khass, and M. E. Mostafa, "Thermal degradation behaviour and chemical kinetic characteristics of biomass pyrolysis using TG/DTG/DTA techniques," Biomass Convers Biorefin, 2023, DOI: 10.1007/s13399-023-03926-2.

[35] S. V. Prabhu et al., "A comparative study on process optimization of betalain pigment extraction from Beta vulgaris subsp. vulgaris: RSM, ANN, and hybrid RSM-GA methods," Biomass Convers Biorefin, 2023, DOI:10.1007/s13399-023-04581-3.

[36] S. Rodrigues, E. S. de Brito, and E. de O. Silva, "Wood Apple—Limoniaacidissima," in Exotic Fruits, S. Rodrigues, E. de Oliveira Silva, and E. S. de Brito, Eds., Academic Press, 2018, pp. 443–446. DOI:10.1016/B978-0-12-803138-4.00060-5

[37] B. Marques, A. Tadeu, J. António, J. Almeida, and J. de Brito, "Mechanical, thermal and acoustic behaviour of polymer-based composite materials produced with rice husk and expanded cork by-products," Constr Build Mater, vol. 239, p. 117851, 2020 .DOI:10.1016/j.conbuildmat.2019.117851